Neurobiology of Disease 73 (2015) 96–105

Contents lists available at ScienceDirect

Neurobiology of Disease

journal homepage: www.elsevier.com/locate/ynbdi

Rapamycin reveals an mTOR-independent repression of Kv1.1 expression during epileptogenesis

Natasha M. Sosanya [a,b], Darrin H. Brager [a], Sarah Wolfe [b,c], Farr Niere [a], Kimberly F. Raab-Graham [a,b,c,*]

[a] Center for Learning and Memory, Department of Neuroscience, University of Texas at Austin, USA
[b] Institute for Cell and Molecular Biology, University of Texas at Austin, USA
[c] Waggoner Center for Alcohol and Addiction Research, University of Texas at Austin University Station C7000, Austin, TX 78712, USA

ARTICLE INFO

Article history:
Received 21 May 2014
Revised 11 August 2014
Accepted 21 September 2014
Available online 28 September 2014

Keywords:
Potassium channels
miRNA
Rapamycin
mTOR
Temporal lobe epilepsy

ABSTRACT

Changes in ion channel expression are implicated in the etiology of epilepsy. However, the molecular leading to long-term aberrant expression of ion channels are not well understood. The mechanistic/mammalian target of rapamycin (mTOR) is a serine/threonine protein kinase that mediates activity-dependent protein synthesis in neurons. mTOR is overactive in epilepsy, suggesting that excessive protein synthesis may contribute to the neuronal pathology. In contrast, we found that mTOR activity and the microRNA miR-129-5p reduce the expression of the voltage-gated potassium channel Kv1.1 in an animal model of temporal lobe epilepsy (TLE). When mTOR activity is low, Kv1.1 expression is high and the frequency of behavioral seizures is low. However, as behavioral seizure activity rises, mTOR activity increases and Kv1.1 protein levels drop. In CA1 pyramidal neurons, the reduction in Kv1.1 lowers the threshold for action potential firing. Interestingly, blocking mTOR activity with rapamycin reduces behavioral seizures and temporarily keeps Kv1.1 levels elevated. Overtime, seizure activity increases and Kv1.1 protein decreases in all animals, even those treated with rapamycin. Notably, the concentration of miR-129-5p, the negative regulator of Kv1.1 mRNA translation, increases by 21 days post-status epilepticus (SE), sustaining Kv1.1 mRNA translational repression. Our results suggest that following kainic-acid induced status epilepticus there are two phases of Kv1.1 repression: (1) an initial mTOR-dependent repression of Kv1.1 that is followed by (2) a miR-129-5p persistent reduction of Kv1.1.

Published by Elsevier Inc.

Introduction

Changes in intracellular signaling often follow neuronal insult or injury leading to a persistent state of neuronal hyperexcitability, as in temporal lobe epilepsy (TLE). The mechanistic/mammalian target of rapamycin (mTOR) is a serine/threonine protein kinase that is overactive following status epilepticus (SE) (Brewster et al., 2013; Zeng et al., 2009). Best characterized for its role in promoting translation of mRNAs, overactive mTOR in neurological disorders is often hypothesized to result in excessive protein synthesis (Hoeffer and Klann, 2010). However, a number of studies suggest that there is a reduction in the expression of voltage-gated ion channels in models of temporal lobe epilepsy (Poolos and Johnston, 2012). Interestingly, activation of mTOR represses the local translation of the delayed rectifier potassium channel Kv1.1 (Raab-Graham et al., 2006). Furthermore, increased seizure susceptibility directly correlates with a decrease in Kv1.1 gene expression (Rho et al., 1999; Smart et al., 1998; Robbins and Tempel, 2012); and overexpression of Kv1.1 eliminates seizures in a rat model of focal epilepsy (Wykes et al., 2012).

Identifying the mechanisms through which mTOR activity represses the translation of ion channel mRNA is important for understanding the cause of epilepsy. RNA-binding proteins and microRNAs can bind to the same target mRNAs and antagonize each other's function (Meisner and Filipowicz, 2011). We recently determined that the microRNA, miR-129-5p, and the RNA binding protein, HuD, compete for binding and translational regulation of Kv1.1 mRNA (Sosanya et al., 2013). When mTOR activity is elevated, Kv1.1 mRNA translation is repressed by miR-129-5p binding. In contrast, when mTOR activity is reduced, miR-129-5p binding is relieved and HuD restores translation (Sosanya et al., 2013). These findings have led us to ask the following questions: (1) Does overactive mTOR following status epilepticus lead to reduced Kv1.1 protein expression? (2) What is the physiological consequence of changes in Kv1.1 protein expression? (3) Are HuD and miR-129-5p, the RNA-binding factors that regulate Kv1.1 mRNA translation, aberrantly expressed in epilepsy?

Herein we report that hippocampal expression of Kv1.1 protein is dynamic over the course of several days following kainic acid-induced

* Corresponding author at: University of Texas at Austin University Station C7000, Austin, TX 78712, USA. Fax: +1 512 475 8000.
E-mail address: Kimberly@mail.clm.utexas.edu (K.F. Raab-Graham).
Available online on ScienceDirect (www.sciencedirect.com).

http://dx.doi.org/10.1016/j.nbd.2014.09.011
0969-9961/Published by Elsevier Inc.

status epilepticus (SE), a critical period during which neuronal remodeling occurs. Expression of Kv1.1 gradually increases over 14 days post-SE. On day 15 there is a dramatic decrease of Kv1.1 expression and Kv1.1 protein continues to decline well below control levels by 21–30 days post-SE. The decrease in Kv1.1 on day 15 is blocked by rapamycin, suggesting that overactive mTOR is responsible. However, the sustained decrease in Kv1.1 expression beyond day 15 is rapamycin-insensitive and consistent with the function of the Kv1.1 repressor miR-129-5p. In line with changes in Kv1.1 protein expression, the threshold for action potential firing in CA1 pyramidal neurons is depolarized at day 14 post-SE when Kv1.1 expression is elevated, and hyperpolarized on day 28–30, when Kv1.1 expression is reduced. Collectively, these data suggest that both mTOR- and miR-129-5p-mediated repressions of Kv1.1 mRNA translation contribute to the neuronal hyperexcitability observed following status epilepticus.

Methods

Animals

Status epilepticus (SE) was induced in 8-week old male Sprague–Dawley rats by intraperitoneal injection of kainic acid (10 mg/kg, Abcam). The behavior of the animals was observed, and seizures were scored according to the Racine scale (Racine, 1972). One hour after the onset of SE (Class V on the Racine scale indicated by rearing followed by falling down as seen for a full motor seizure), seizures were terminated by subcutaneous injection of sodium pentobarbital (PB; 30 mg/kg). Control rats received the appropriate volume of saline vehicle followed by PB 1 h later. For rapamycin (LC Laboratories) injection, we followed a modified protocol reported by Meikle et al. (Meikle et al., 2008). Rapamycin was dissolved at 50 mg/ml in ethanol and stored at −20 °C. Before each administration, rapamycin was diluted in 7% Tween 80, 7% polyethylene glycol 400 (PEG-400) and water to final 6% ethanol (Brewster et al., 2013). Rapamycin or vehicle (7% Tween 80, 7% PEG-400, 6% ethanol) was given at 6 mg/kg intraperitoneally every 4 days. All animal experiments were performed in accordance with guidelines approved by the Institutional Animal Care and Use Committee (IACUC) at The University of Texas-Austin.

Continuous video monitoring

Kainic acid-injected rats (KA) were video monitored from day 2 to day 21 post-SE and were scored from 7 am to 3 pm (Fig. 1) or from 4:30–7 pm (Fig. 7) by an individual blind to the condition. Behavioral seizures ranging from Class III (dog shake) to Class V (full rearing followed by falling down) on the Racine scale were scored.

Slice preparation

Hippocampal slices were prepared from control and post-SE rats as described previously (Shin et al., 2008). Briefly, animals were anesthetized using a lethal dose of ketamine and xylazine. Once deeply anesthetized, animals were perfused intracardially with ice-cold modified ACSF containing (in mM) 210 sucrose, 2.5 KCl, 1.2 NaH_2PO_4, 25 $NaHCO_3$, 0.5 $CaCl_2$, 7.0 $MgCl_2$, and 7.0 dextrose bubbled with 95%O_2/5%CO_2. The brain was removed and bisected along the midline. One hemisphere was used for slice preparation for electrophysiological recording and the other hemisphere was used for biochemical analyses (see Western blot analysis, immunohistochemistry, and RT-qPCR). The hemisphere was mounted and 350 μm thick slices were made using a microtome (Vibratome, St. Louis MO). Slices were placed in a holding chamber filled with ACSF containing (mM): 125 NaCl, 2.5 KCl, 1.25 NaH_2PO4, 25 $NaHCO_3$, 2 $CaCl_2$, 2 $MgCl_2$, and 12.5 dextrose warmed to 35 °C for 20 min and then placed at room temperature for <6 h until needed for recording.

Electrophysiology

Slices were placed individually as needed into a submerged recording chamber continuously perfused with control extracellular saline (see below). Slices were viewed with a Zeiss Axioskop using infrared video microscopy and differential interference contrast (DIC) optics. For all recordings, the ACSF solution contained (mM): 125 NaCl, 3 KCl, 1.25 NaH_2PO_4, 25 $NaHCO_3$, 2 $CaCl_2$, 1 $MgCl_2$, and 12.5 dextrose and was bubbled continuously with 95%O_2/5% CO_2 at 31–33 °C. Fast glutamatergic and GABAergic synaptic transmissions were blocked by a combination of 20 μM DNQX, 50 μM AP5, 2 μM gabazine, and 5 μM CGP55845.

Patch pipettes were pulled from borosilicate glass and had a resistance of 4–8 MΩ when filled with the internal recording solution containing (in mM): 120 potassium gluconate, 20 KCl, 10 HEPES, 4 NaCl, 4 MgATP, 0.3 Na-GTP and 7 phosphocreatine (pH 7.3 with KOH). Whole cell recordings were made from the soma of CA1 pyramidal neurons using a Multiclamp 700A or Dagan BVC in current clamp mode. Series resistance was monitored throughout the recording, and experiments in which the series resistance exceeded 30 MΩ were discarded.

Data acquisition and analysis

Data were sampled at 40 kHz, filtered at 5 kHz and digitized by an ITC-18 interface connected to computer running Axograph X. Data analyses were performed with Axograph X.

Western blot analysis

The hippocampus was immediately dissected from the hemisphere of the brain not used for physiology (see Slice preparation). Synaptoneurosomal (SN) protein and RNA were prepared from the hippocampus as outlined (Sosanya et al., 2013). Proteins were separated by SDS-PAGE, transferred to nitrocellulose, and blocked with 5% milk + Tween 20. Blots were then probed with antibodies against Kv1.1 (1:500; Neuromab K36/15), p-mTOR (1:500, Cell Signaling 5536), mTOR (1:500, Invitrogen AHO1232), HuD (1:500; Millipore AB5971), and tubulin (1:2000; Abcam ab15246). Anti-p-mTOR (rabbit) and anti-total mTOR (mouse) were probed and detected with an anti-mouse-IR-Dye 800 (1:2000; LICOR 926-32210) and anti-rabbit-Alexa680 secondary antibodies (1:2000; Invitrogen A-21084). Dual color imaging for within blot analysis for P-mTOR and total mTOR as well as Kv1.1 and tubulin was performed on the LICOR Odyssey imaging system. All Western blots were imaged such that pixel intensities within the band were in the linear range, as indicated by LICOR detection software. Densitometry of the immunoreactive bands was performed using the NIH Image software (Image J) using the profile function.

Immunohistochemistry

Control and KA-injected rats were perfused with ice cold PBS and post-fixed with 4% formaldehyde overnight at 4 °C. 80 μm thick coronal sections of the hippocampus were taken on a vibratome and placed free floating in PBS. Hippocampal slices with similar morphology were double stained for Kv1.1 and tubulin. Slices were blocked overnight at 4 °C in blocking solution (10% goat serum with 0.3% Triton X-100 in PBS) and then incubated with mouse-anti-Kv1.1 (1:200, Neuromab K36/15) and rabbit anti-tubulin (1:200, Abcam) overnight at RT in blocking solution. The following day, slices were washed in PBS for 1 × 10 min, 1 × 30 min, and 1 × 40 min and then incubated in blocking solution for 2 h at RT. Slices were then incubated overnight at 4 °C in secondary antibody followed by same washing protocol as above. Once mounted on glass slides slices were imaged on a Leica SP5 confocal microscope (Leica DM6000 CFS 20×/0.70 objective HC PL APO 0.17/C). Images were acquired based on relative tubulin signal and the same settings in the same imaging session. A z-series of 20, 1 μm sections were collected

and projected. An equal size region of interest (ROI) box was drawn in either the CA1 or CA3 regions and the ratio of Kv1.1 to tubulin signal was measured. Quantification was done using the NIH ImageJ software plugin T-functions Ratio ROI Manager.

Reverse transcription-quantitative PCR (RT-qPCR)

SN RNA was isolated using Zymogen Direct-zol RNA miniprep kit according to the manufacturer's directions. RT-quantitative PCRs for miR-129-5p, miR-145-5p, or 5S rRNA were done using the miRCURY LNA Universal RT microRNA PCR kits (Exiqon; universal cDNA #203300 and Sybr green master mix #203450) using specific primers (Exiqon) starting with 22 ng of total RNA according to the manufacturer's directions and previously described and verified by Northern blot analysis (Sosanya et al., 2013). RT-qPCRs for Kv1.1 and GAPDH were performed using the iQ cDNA synthesis (170-8890) and SYBR green (170-8880) kits from Biorad following the manufacturer's directions (Raab-Graham et al., 2006; Sosanya et al., 2013). Fold changes were calculated as outlined (Raab-Graham et al., 2006; Sosanya et al., 2013). Relative ratios were calculated by the model as previously described (Pfaffl, 2001) and calculated by the equation: ratio = (2ΔCPtarget (control-sample) ÷ 2ΔCPreference (control-sample)), where CP is the threshold cycle, the target is the transcript of interest, and the reference is either 5S rRNA or GAPDH. Internal control (5S rRNA or GAPDH), no-RT control, and miR-129-5p RT-PCR were run in parallel and in duplicate. Validation of product was determined by melt curve analysis at the completion of the PCR amplification. Ct values of duplicates were averaged and compared between animals.

Statistical analyses

All data are expressed as mean ± S.E.M. Statistical comparisons were made using one-way or two-way ANOVA followed by Tukey–Kramer or Dunnett's multiple comparisons post-hoc test or Student's *t*-test (paired or unpaired as appropriate) with Prism software (GraphPad). Linear fits and correlations were made using Prism. Data were considered statistically significant if $p < 0.05$.

Results

Behavioral seizures increase between 15 and 21 days post-SE

The kainic acid (KA) model of TLE is useful for identifying molecular changes that occur during epileptogenesis leading to recurrent, chronic seizures (Aronica et al., 1997; Friedman et al., 1997; Grooms et al., 2000; Misonou et al., 2006; Mohapatra et al., 2009; Schauwecker et al., 2000; Tongiorgi et al., 2004). Shortly after periods of intense activity, neurons may undergo homeostatic changes in ion channel function and/or expression that can reduce the overall activity of the neuron (Fan et al., 2005; Narayanan and Johnston, 2010; Shin et al., 2008; Baram, 2012; Krook-Magnuson et al., 2013; Patterson et al., 2014). In some cases these changes are transient, and what follows are persistent states of neuronal hyperexcitability, ultimately leading to the onset of recurrent seizure activity (Sun et al., 2013). To determine when these dynamic changes in ion channel expression and/or function may occur, we first determined the onset of seizure activity, as measured by behavioral seizures. Rats were continuously video monitored and behavioral seizures ranging from Class III–V (Racine, 1972) were scored from 2 to 21 days post-SE. We found that although seizure number remained low for the first 2 weeks post-SE, there was a sharp increase in seizure occurrence between days 14 and 15. Furthermore, seizure frequency continued to climb from day 15 to day 21, where seizure number became significantly higher when compared to all other time points (Fig. 1).

Increased mTOR activity corresponds to peak number of behavioral seizures

Activation of mTOR is elevated in several models of TLE, including KA (Brewster et al., 2013; Zeng et al., 2009). Increases in mTOR activity repress the expression of several voltage-gated ion channels, including Kv1.1 (Brewster et al., 2013; Lee et al., 2011; Raab-Graham et al., 2006; Sosanya et al., 2013). In light of the behavioral seizure progression (Fig. 1), we set out to determine when mTOR became hyperactive post-SE. To address this question, we measured mTOR activity in the hippocampus of control and KA rats at time points that corresponded to observed behavioral seizure activity. Synaptoneurosomes isolated from the hippocampus were subjected to Western blot analysis for phosphorylated-mTOR (p-mTOR) and total mTOR. The ratio of p-mTOR/mTOR served as a readout for mTOR activity. Consistent with behavioral seizure occurrence, mTOR activity was significantly depressed 14 days post-SE. This was followed by a sharp, significant increase 15 days post-SE which remained elevated through 30 days (0 day: 1.00 ± 0.05, 2 days post-SE: 0.86 ± 0.07, 5 days post-SE: 1.07 ± 0.02; 14 days post-SE: 0.52 ± 0.16, 15 days post-SE: 1.19 ± 0.17; control: 1.00 ± 0.06, 21–30 days post-SE: 1.88 ± 0.275; Figs. 2A–B). The change in p-mTOR/mTOR ratio was not due to changes in total mTOR expression (Fig. S1). These data suggest a switch in mTOR activity between day 14 post-SE, when mTOR activity is 38.7% lower than control, and days 21–30 post-SE, when mTOR activity is 37% higher than control (Fig. 1C). Furthermore, the onset of hyperactive mTOR correlated with the significant increase in behavioral seizure occurrence.

Bidirectional changes in Kv1.1 expression in TLE

The overexpression of Kv1.1 can provide protection against seizures in drug-resistant, focal, neocortical epilepsy (Wykes et al., 2012). We therefore asked if Kv1.1 expression underwent changes that paralleled changes in seizure and mTOR activity following SE. As predicted, Kv1.1 expression gradually increased over 14 days post-SE, peaking at ~71% above control levels and precipitously dropping back to control levels by 15 days (0 day SA + PB: 1.00 ± 0.03, 2 days post-SE: 1.07 ± 0.08, 5 days post-SE: 1.27 ± 0.09; 14 days post-SE: 1.77 ± 0.12; 15 days post-SE: 0.98 ± 0.05; Fig. 3A). By 21–30 days post-SE, Kv1.1 levels were further reduced by ~50% relative to control (control SA + PB: 1.00 ± 0.06; 21–30 day post-SE: 0.54 ± 0.15; Fig. 3B). A comparison

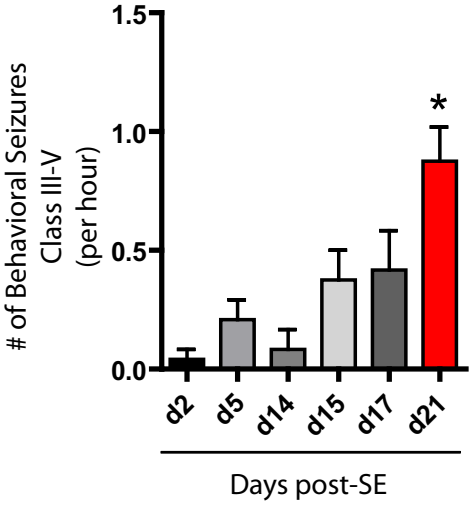

Fig. 1. Number of behavioral seizures increases at 21 days post-SE. Three KA-injected rats were placed in an isolated room where they were continuously video monitored for the progression of behavioral seizures until day 21 post-SE. KA rats were scored by number of behavioral seizures ranging from Class III–V by an individual blind to treatment. * day 2 to day 21: $p < 0.01$; day 5 to day 21: $p < 0.01$; day 14 to day 21: $p < 0.01$; day 15 to day 21: $p < 0.05$; day 17 to day 21: $p < 0.05$ by one-way ANOVA, Newman–Keuls post hoc test.

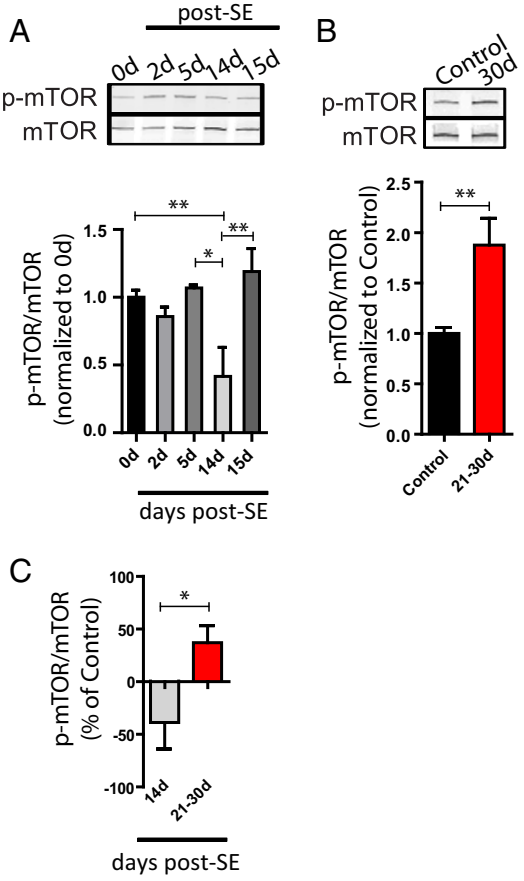

Fig. 2. Differential mTOR activity occurs post-SE. (A) Hippocampal SN protein was isolated from 0 day (saline + PB, euthanized 1 day post-injection) and kainic acid-(KA + PB) treated animals at 2, 5, 14, and 15 days post-SE. Top, representative Western blot of a SDS-PAGE gradient gel probed with antibodies against p-mTOR and mTOR. Quantification of p-mTOR/mTOR levels normalized by tubulin, relative to 0 day is shown below. 0 day: n = 14, 2 days post-SE: n = 6, 5 days post-SE: n = 5, 14 days post-SE: n = 3, 15 days post-SE: n = 3; * < 0.05, ** < 0.01 by one-way ANOVA, Dunnett's post hoc test. (B) Hippocampal SN protein was isolated from control (saline + PB, euthanized 21–30 days post-injection) and kainic acid-(KA + PB) treated animals 21–30 days post-SE. Top, representative Western blot of a SDS-PAGE gradient gel probed with antibodies against p-mTOR and mTOR. Quantification of p-mTOR/mTOR normalized by tubulin and relative to control is shown below. Control: n = 9; 21–30 day post-SE: n = 9; * < 0.05. (C) Percent of control for p-mTOR/mTOR of 14 days and 21–30 days post SE animals from Figs. 2A–B is shown. * < 0.05, significance determined by Student's *t*-test for both B and C. Error bars are SEM.

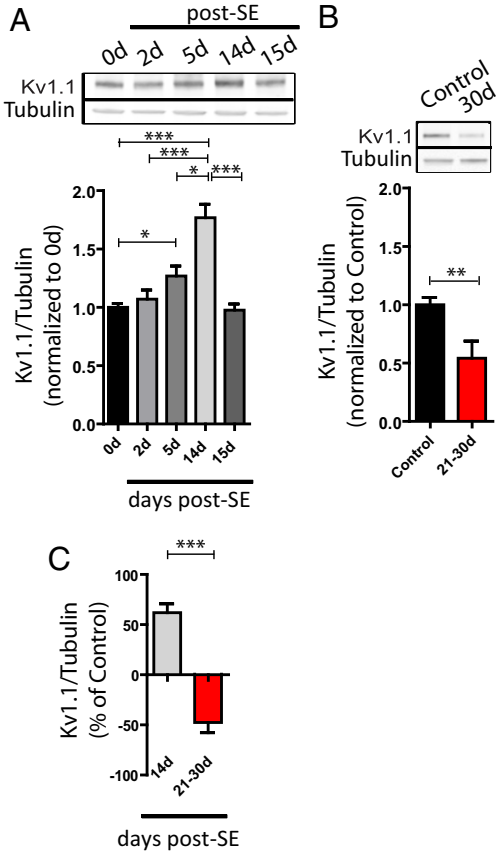

Fig. 3. Kv1.1 protein levels peak at 14 days post-SE, followed by a significant drop at 21–30 days post-SE. (A) Hippocampal SN protein was isolated from 0 day (saline + PB, euthanized 1 day post-injection) and kainic acid-(KA + PB) treated animals 2, 5, 14, and 15 days post SE. Top, representative Western blot of a SDS-PAGE gradient gel probed with antibodies against Kv1.1 and tubulin. Quantification of Kv1.1 signal normalized by tubulin levels and relative to 0 day is shown below. *p < 0.05, ***p < 0.005 by one-way ANOVA, Tukey's post hoc test. 0 day: n = 16, 2 days post-SE: n = 6, 5 days post-SE: n = 5, 14 days post-SE: n = 4, 15 days post-SE: n = 3, 21–30 days post-SE: n = 5. Error bars represent SEM. (B) Hippocampal SN protein was isolated from control (saline + PB, euthanized 21–30 days post-injection) and kainic acid-(KA + PB) treated animals 2, 5, 14, and 15 days post SE. Top, representative Western blot of a SDS-PAGE gradient gel probed with antibodies against Kv1.1 and tubulin. Quantification of Kv1.1 signal normalized by tubulin levels and relative to control is shown below. **p < 0.001, significance determined by Student's *t*-test. Control: n = 7; 21–30 days post-SE: n = 5. Error bars represent SEM. (C) Percent of control for Kv1.1/tubulin of 14 days and 21–30days post-SE animals from Figs. 3A–B is shown. *** < 0.005, significance determined by Student's *t*-test. Error bars are SEM.

of Kv1.1 protein revealed an opposite switch in Kv1.1 levels from 14 days to 21–30 days post-SE compared to the change in mTOR activity (Fig. 3C). These results are consistent with mTOR-mediated suppression of Kv1.1 expression. The drop in Kv1.1 expression may contribute to the gradual increase in behavioral seizures from day 15 to day 21 post-SE as mTOR activity increases.

To determine the regional distribution of the changes in Kv1.1 expression post-SE, we stained hippocampal sections for Kv1.1 from control and KA rats 14 and 30 days post-SE. In agreement with our Western blot results, we found that the intensity of Kv1.1 staining increased by ~50% in both areas CA1 and CA3 14 days post-SE when compared to day 0 (Figs. 4A, C). By 30 days Kv1.1 staining was reduced by ~60% in CA1 and ~45% in CA3 of KA rats compared to control rats (Figs. 4B, D).

Dynamic changes in Kv1.1 expression post-SE alter the threshold for action potential firing

In cortical neurons, dynamic changes in Kv1 channels reset the threshold for action potential firing (V_{TH}) (Higgs and Spain, 2011). Based on our biochemical results, we hypothesized that an increase on day 14, and a decrease on day 28, in Kv1.1 expression would be accompanied by a depolarization and hyperpolarization of V_{TH} respectively. To test if V_{TH} is altered, we recorded single action potentials (APs) elicited in CA1 pyramidal neurons from KA- and saline-injected rats at 13–14 days post-SE, when Kv1.1 expression is highest, and 21–30 days post-SE, when Kv1.1 expression is reduced. Single APs were elicited using small amplitude, 100-msec current injections (which is sensitive to Kv1.1 expression) and large amplitude, 2-msec current injections (which are not sensitive to Kv1.1 expression) (Higgs and Spain, 2011). The amplitude of the 100-msec current pulse was adjusted so that a single action potential occurred in the middle (~50 msec latency) of the current injection. Using the 100-msec injection, we found that V_{TH} in CA1 pyramidal neurons was significantly depolarized at 5 days and 13–14 days post-SE (Figs. 5 and S2). In contrast, V_{TH} at 21–30 days post-SE in CA1 pyramidal neurons was hyperpolarized by ~3 mV compared to control and ~9 mV compared to 13–14 days post-SE (Figs. 5A and B). There was no significant difference in V_{TH} measured with the 2-msec current injections in control and post-SE animals (Figs. 5C and D). These results are consistent with our observed changes in Kv1.1 expression.

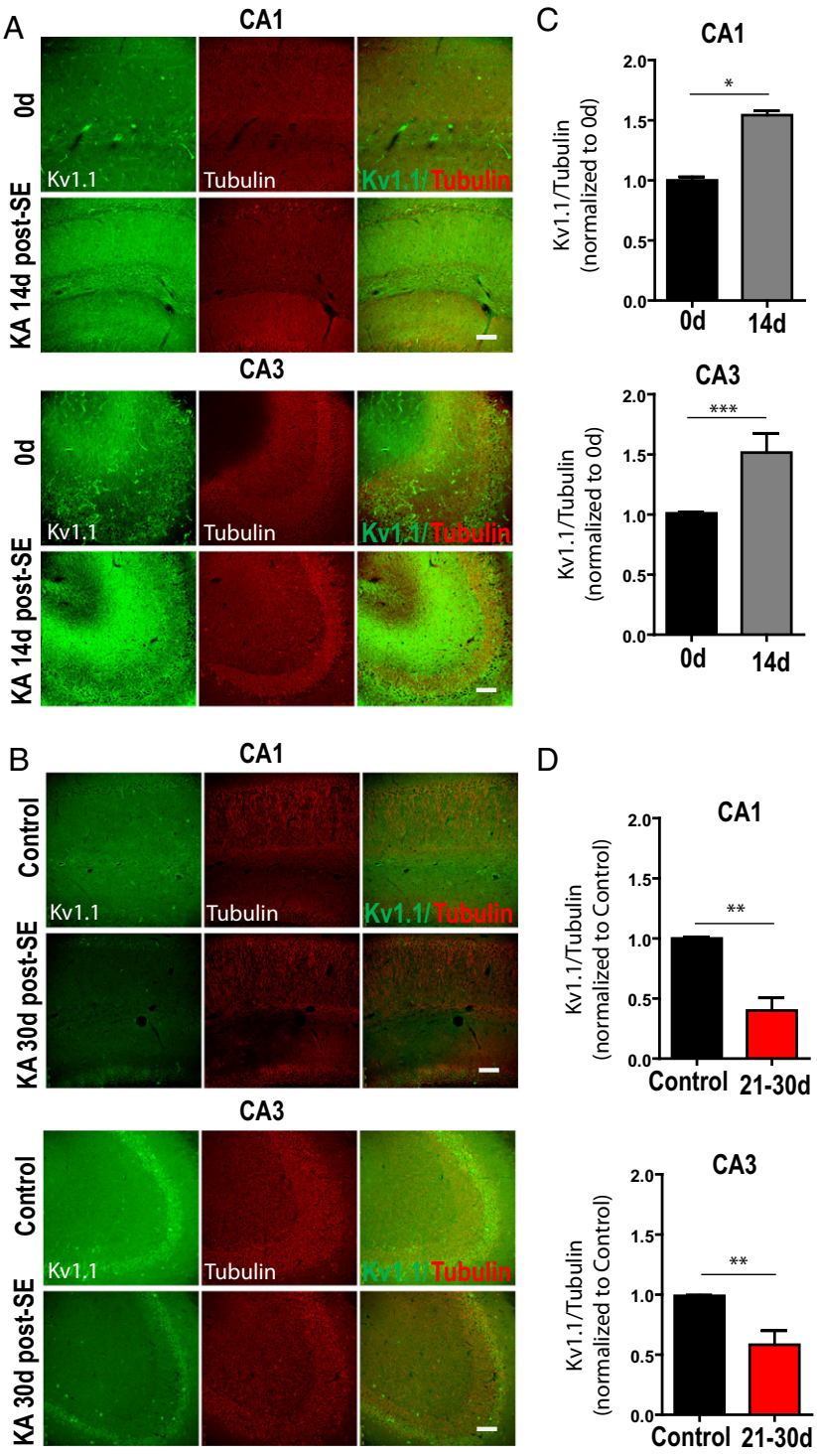

Fig. 4. Kv1.1 protein increases 14 days post-SE and decreases 30 days post-SE in hippocampal CA1 and CA3 regions. (A) Coronal slices from control and 14 days post-SE rats were immunostained for Kv1.1 and tubulin (volume control) followed by imaging with the Leica SP5 confocal microscope 20× objective. Representative slices CA1 and CA3 regions from 14 days post-SE rats are shown. Kv1.1 is indicated by green signal and tubulin is indicated by red signal. Scale bar = 100 μm. (B) Coronal slices from control and 21–30 days post-SE rats were immunostained for Kv1.1 and tubulin (volume control) followed by confocal microscopy with a 20× objective. Representative slices of CA1 and CA3 regions from 30 days post-SE rat are shown. Kv1.1 is indicated by green signal and tubulin is indicated by red signal. Scale bar = 100 μm. (C) Quantification of CA1 and CA3 regions at 14 days post-SE. Kv1.1/tubulin is normalized to control. 0 day: n = 4, 14 days: n = 4. (D) Quantification of CA1 and CA3 regions at 21–30 days post-SE. Kv1.1/tubulin is normalized to control. control: n = 4, 21–30 day: n = 4.

To test whether the changes in Kv1 expression contributed to the observed differences in V_{TH}, we bath applied a low concentration of 4-aminopyridine (4-AP, 50 μM), a potassium channel blocker. 4-AP significantly hyperpolarized V_{TH} measured with 100-msec injections at all time points except 21–30 days post-SE, when Kv1 expression is lowest (Figs. 5A, B and D). V_{TH} measured with 2-msec injections was insensitive to 4-AP in both control and post-SE animals. These data support the hypothesis that an increase in functional expression Kv1.1-containing channels occurs after SE peaking at 14 days post-SE. This increase is transient and is reduced by 21–30 days post-SE. The loss of

functional Kv1.1-containing channels at 21–30 days post-SE renders CA1 pyramidal neurons hyperexcitable by reducing the threshold for action potential firing.

Rapamycin treatment reveals an mTOR-independent change in seizure and Kv1.1 expression

The mTORC1 inhibitor rapamycin is effective at reducing seizure activity (Zeng et al., 2009; Brewster et al., 2013; Wong, 2012). In addition, we found that acute rapamycin treatment increases the local translation of Kv1.1 mRNA in neuronal hippocampal dendrites (Raab-Graham et al., 2006; Sosanya et al., 2013). Based on these data, we hypothesized that rapamycin treatment should increase Kv1.1 expression and reduce seizure frequency. We chose to start rapamycin treatment on day 14 post-SE when mTOR levels were low with the idea that we will block the increase in mTOR activity and concomitant reduction of Kv1.1 expression at day 15.

Consistent with previous results, rapamycin reduced seizure number by ~60 and ~50% by days 17 and 21, respectively (Fig. 6B). Despite this reduction in seizure occurrence, there remained an mTOR-independent increase in seizure frequency between days 17 and 21 (Fig. 6C, KA: 9.00 ± 3.5, $p < 0.01$ KA + Rapa: 4.2 ± 1.8, $p < 0.05$). To confirm that rapamycin effectively blocked mTOR activation, we measured the p-mTOR/total mTOR ratio in hippocampi of KA- and rapamycin-treated KA rats. Rapamycin reduced mTOR activity by ~50% at both days 17 and 21 post-SE (Figs. 6D–E; mTOR Rapa: 1.08 ± 0.26). Interestingly, although Kv1.1 expression remained elevated at 17 days post-SE with rapamycin, by 21 days post-SE with rapamycin Kv1.1 expression was lower than untreated KA rats (Figs. 6D–E; Kv1.1 Rapa: 0.54 ± 0.09). These data suggest a secondary, mTOR-independent mechanism that represses Kv1.1 protein expression.

Increased expression of the microRNA miR-129-5p contributes to the late phase repression of Kv1.1 expression

The rapid rise in mTOR activity occurring between days 14 and 15 post-SE corresponds to a drop in Kv1.1 expression. By day 21 post-SE, Kv1.1 expression remains low even when mTOR is blocked by rapamycin. What is the molecular mechanism that maintains the reduced Kv1.1 expression in TLE? Changes in transcription of many mRNAs occur during epileptogenesis (Ozbas-Gerçeker et al., 2006). To determine if changes in Kv1.1 protein expression are due to an effect on transcription, we measured Kv1.1 mRNA levels by RT-qPCR. We found that levels of Kv1.1 mRNA change after SE in a pattern opposite to Kv1.1 protein: when Kv1.1 protein levels peak at 14 days post-SE, Kv1.1 mRNAs are reduced by ~50% (Fig. 7A; control: 1.00 ± 0.06, 2 days post-SE: 0.84 ± 0.03, 5 days post-SE: 1.06 ± 0.11, 14 days post-SE: 0.49 ± 0.14, 15 days post-SE: 1.05 ± .13). Furthermore, as mTOR activity increased and Kv1.1 protein levels dropped, Kv1.1 mRNA expression returned to control levels (Figs. 7A and B). This inverse relationship between Kv1.1 protein and mRNA suggests that transcription rates are likely to be relatively constant throughout epileptogenesis and that the bidirectional changes in Kv1.1 protein levels may be regulated at the translational level.

Recently, our laboratory determined that the microRNA, miR-129-5p negatively regulates the expression of Kv1.1 in neurons when mTOR is active and that the RNA-binding protein HuD positively regulates the translation of Kv1.1 mRNA when mTOR is inhibited (Sosanya et al., 2013). With acute inhibition of mTOR activity, the levels of the RNA-binding factors do not change; however, several HuD mRNA

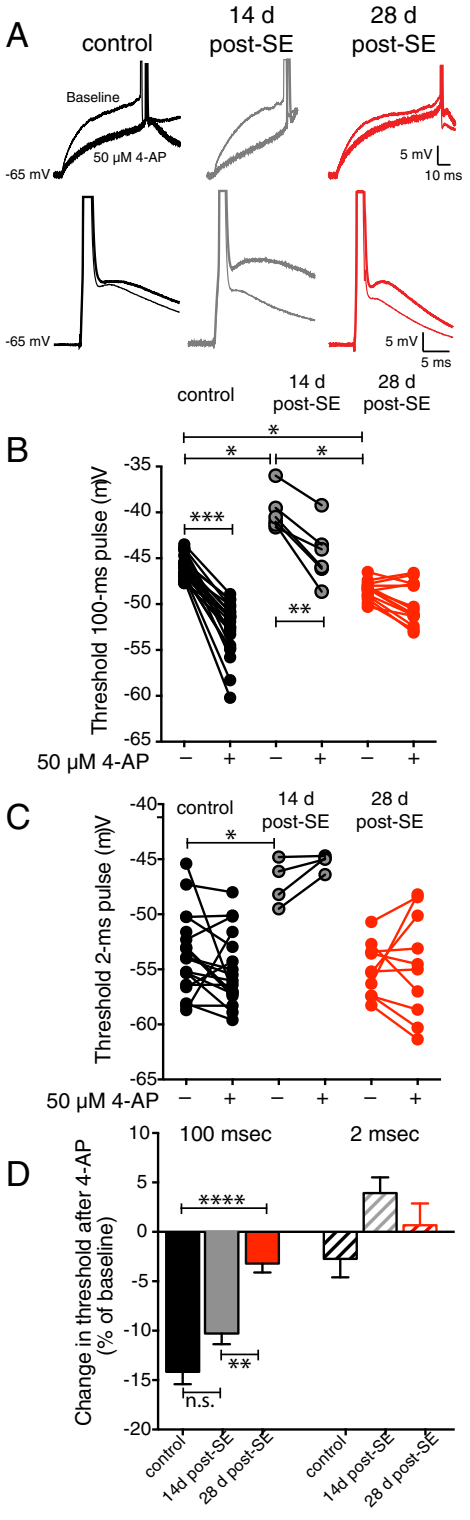

Fig. 5. Action potential threshold (V_{TH}) bidirectionally changes in CA1 pyramidal neurons expressing TLE. (A) Voltage recordings showing a single action potential elicited by a 100-msec (top) and 2-msec (bottom) current injections before (thin line) and after (thick line) application of 50 μM 4-AP from control (black), 13–14 days post-SE (gray), and 21–30 days post-SE (red) CA1 neurons. (B) The threshold of action potentials elicited by 100-msec current injection is significantly depolarized at 14 days post-SE and hyperpolarized at 21–30 day post-SE relative to control. 4-AP application significantly hyperpolarized V_{TH} in control and 14 days post-SE but not 21–30 days post-SE neurons. $^{**}p < 0.01$, $^{****}p < 0.001$ by one-way ANOVA. (C) There is no significant difference in action potential threshold elicited during the 2-msec steps between control and 21–30 days post-SE CA1 neurons. 4-AP has no significant effect on action potential threshold in either control or 21–30 days post-SE neurons. (D) Summary data showing that 4-AP significantly hyperpolarized action potential threshold in control and 14 days, but not 21–30 days post-SE neurons for the 100-msec current injection. $^{**}p < 0.01$ compared to 14 days post-SE. $^{****}p < 0.001$ compared to 21–30 days post-SE.

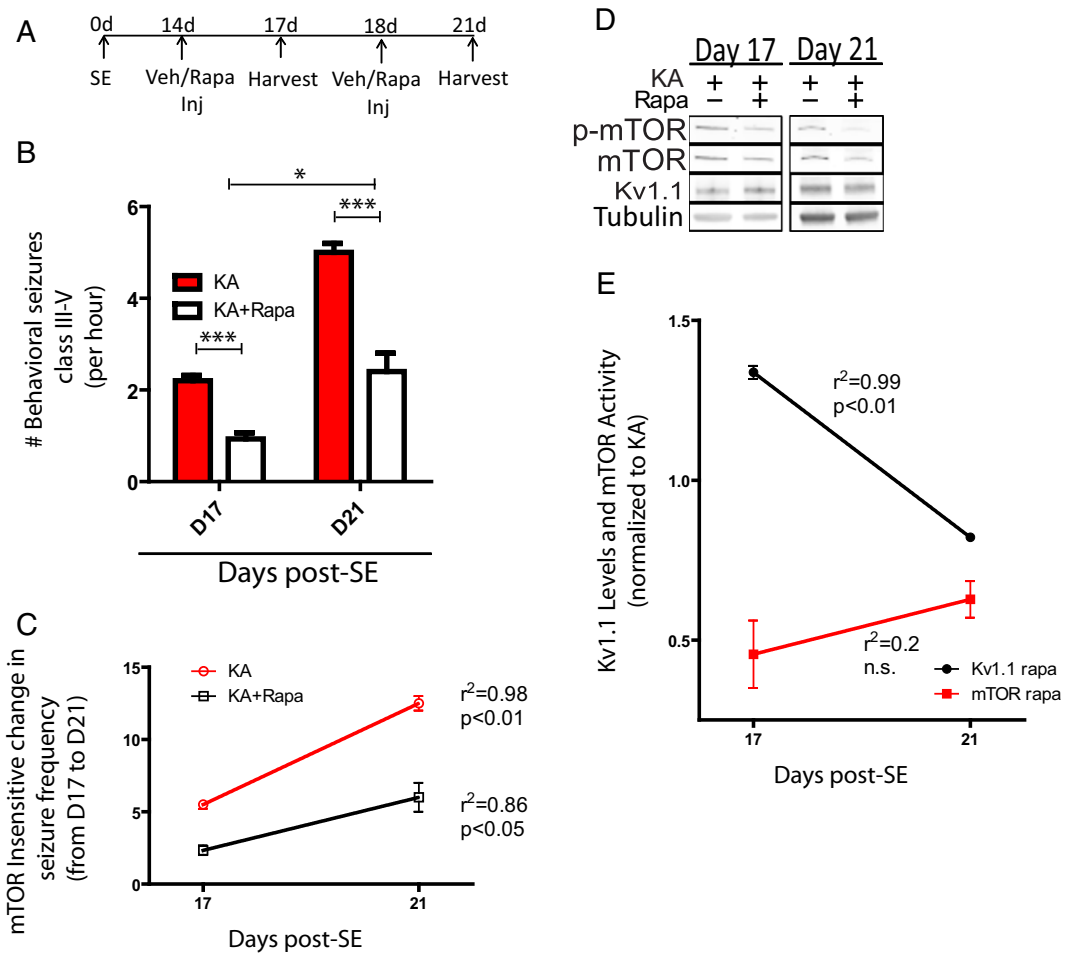

Fig. 6. mTOR inhibits Kv1.1 in early but not late TLE. (A) Timeline indicating date of SE (at 0 day), vehicle or rapamycin injection (at 14 days post-SE) followed by harvest of hippocampal synaptoneurosomal protein (at 17 days post-SE) or a second injection with vehicle or rapamycin (at 18 days post-SE) followed by harvest of hippocampal synaptoneurosomal protein (at 21 days post-SE). (B) Video monitoring of KA rats indicate that rapamycin injection inhibits ~50% of behavioral seizure activity (Class III–V) at 17 and 21 days post-SE. * < 0.05. Error bars are SEM. (C) Plot demonstrating rise in seizure activity in both KA rats and rapamycin-treated KA rats between day 17 and 21. Note the rise in seizure activity in all groups is significantly different between 17 and 21 days. KA: $p < 0.01$; KA + rapa: $p < 0.05$ as determined by linear regression. (D) Hippocampal SN protein was isolated from KA animals 17 days and 21 days post-SE, and 3 days post vehicle or rapaymcyin injection. Representative Western blots of a SDS-PAGE gradient gel probed with antibodies against p-mTOR, mTOR, Kv1.1, and tubulin. Note the decrease in p-mTOR and the increase in Kv1.1 expression when KA rats are treated with rapamycin at 17 days. In contrast, at 21 days p-mTOR remains reduced with rapamycin treatment while Kv1.1 expression returns to KA levels. (E) Plot demonstrating the mTOR-independent change in Kv1.1 expression in KA rats treated with rapamycin between 17 and 21 days post-SE ($r^2 = 0.99$; $p < 0.01$) whereas the ratio of p-mTOR over total mTOR does not change over time ($R^2 = 0.02$; n.s. = not significant). Error bars represent SEM. KA: n = 2; KA + Rapa: n = 2. Error bars represent SD.

targets degrade, allowing HuD to bind to Kv1.1 mRNA and promote its translation (Sosanya et al., 2013). Shifting the balance of either of these RNA-binding factors (i.e. increasing miR-129-5p levels or decreasing HuD levels) favors the repression of Kv1.1 mRNA translation. To determine if a shift in the balance between these RNA binding factors occurs in TLE, we measured miR-129-5p and HuD levels. We found that both miR-129-5p and HuD levels remain unchanged at both 14 and 15 days post-SE (Figs. 7C, D). However, by 21–30 days post-SE, miR-129-5p levels increased by ~76%, while HuD levels remained constant (Figs. 7E, F). This change is specific for miR-129-5p, as expression of miR-145-5p does not change. Taken together these data suggest that an increase in miR-129-5p expression with no change in HuD favors repression of Kv1.1 mRNA translation.

To determine if rapamycin affects the expression of miR-129-5p we compared KA rats to KA rats treated with rapamycin. Unexpectedly, miR-129-5p levels are significantly higher in hippocampi isolated from KA rats treated with rapamycin 21 days post-SE compared to KA treatment alone, with no change in miR-145-5p (Fig. 7H; Day 21: KA: 1.00 ± 0.25, KA + Rapa: 2.02 ± 0.19). There was no effect of rapamycin on miR-129-5p levels at 17 days post-SE (Fig. 7G). These results are consistent with the observed reduction in Kv1.1 protein in the presence of rapamycin at 21 days post-SE. Together these data suggest that increased levels of miR-129-5p underlie the late phase, post-SE repression of Kv1.1 translation.

Discussion

Many ion channels are dynamically regulated during epileptogenesis (Baek et al., 2014; Child and Benarroch, 2014; Lee et al., 2014; Monaghan et al., 2008; Poolos and Johnston, 2012; Powell et al., 2014) and a growing number are linked to changes in mTOR activity (Brewster et al., 2013; Lee et al., 2011; Raab-Graham et al., 2006). We recently described a mechanism by which mTOR can influence the expression of Kv1.1 by regulating two RNA-binding factors, miR-129-5p and HuD (Sosanya et al., 2013). In this study, we found that hippocampal expression of Kv1.1 is elevated 14 days post-SE. This increase in Kv1.1 expression is likely due to the low levels of mTOR activity, a condition that favors the release of miR-129-5p repression by the RNA binding protein HuD (Fig. 8, middle panel). In contrast, miR-129-5p levels are elevated 21–30 days post-SE, shifting the balance toward

Kv1.1 mRNA repression, thus leading to reduced Kv1.1 expression and a hyperpolarized action potential threshold (Fig. 8, right panel, Late TLE, red arrow). This shift may contribute to CA1 pyramidal neuron hyperexcitability, during a time when recurrent, spontaneous behavioral seizures occur (Fig. 1). Our findings support a bimodal, posttranscriptional regulation of Kv1.1-containing delayed rectifier potassium channels by mTOR and miR-129-5p in a model of TLE (Fig. 8). In the pilocarpine model of epilepsy, Brewster et al. found that the chronic use of the mTORC1 inhibitor rapamycin did not reverse interictal epileptiform activity or increase the levels of Kv1.1 in the hippocampus of epileptic rats (Brewster et al., 2013). Our findings may explain these results by demonstrating a second mechanism that represses Kv1.1 expression, independent of mTOR activity. We found that despite long-term treatment with rapamycin, miR-129-5p levels increase post-SE resulting in the repression of its targets such as Kv1.1.

The initial rise in ion channel expression in TLE, reported in this study for Kv1.1 and previously seen with HCN channels (Shin et al., 2008), may help explain the reduced numbers of behavioral seizures during the latent period. However, the failure to sustain elevated levels of these channels may lead to chronic epilepsy. The concurrent increase in mTOR activity coincides with the decline in channel expression. Why mTOR activity fails to renormalize in TLE is an open question. Interestingly, a recent report suggests that mTOR activity also inhibits the expression of the homeostasis protein polo-like kinase 2 (PLK2) in a neonatal seizure model (Sun et al., 2013). Although the mechanism of repression has not been established, it has been shown that PLK2 down regulates mTOR signaling through its interaction with the upstream inhibitor tuberous sclerosis complex 1 (Matthew et al., 2009). Collectively, these studies suggest that mRNAs repressed by mTOR activity may play a critical role in epileptogenesis. However, those mRNAs that undergo a second mode of repression, like miR-129-5p regulation of Kv1.1, may explain an mTOR-insensitive phase of TLE.

In summary, increased or decreased expression of RNA binding factors, which alters the competition for target ion channel mRNAs, can shift the balance between repression and promotion of translation and lead to diseases. The present study shows that following SE, elevated expression of miR-129-5p that is not properly counter balanced by HuD leads to reduced Kv1.1 expression and hyperpolarization of action potential threshold resulting in CA1 pyramidal neuron hyperexcitability. These studies provide a unique model of regulating ion channel expression which may be relevant to other mTOR-related diseases that present epilepsy, such as tuberous sclerosis complex, fragile X syndrome, and

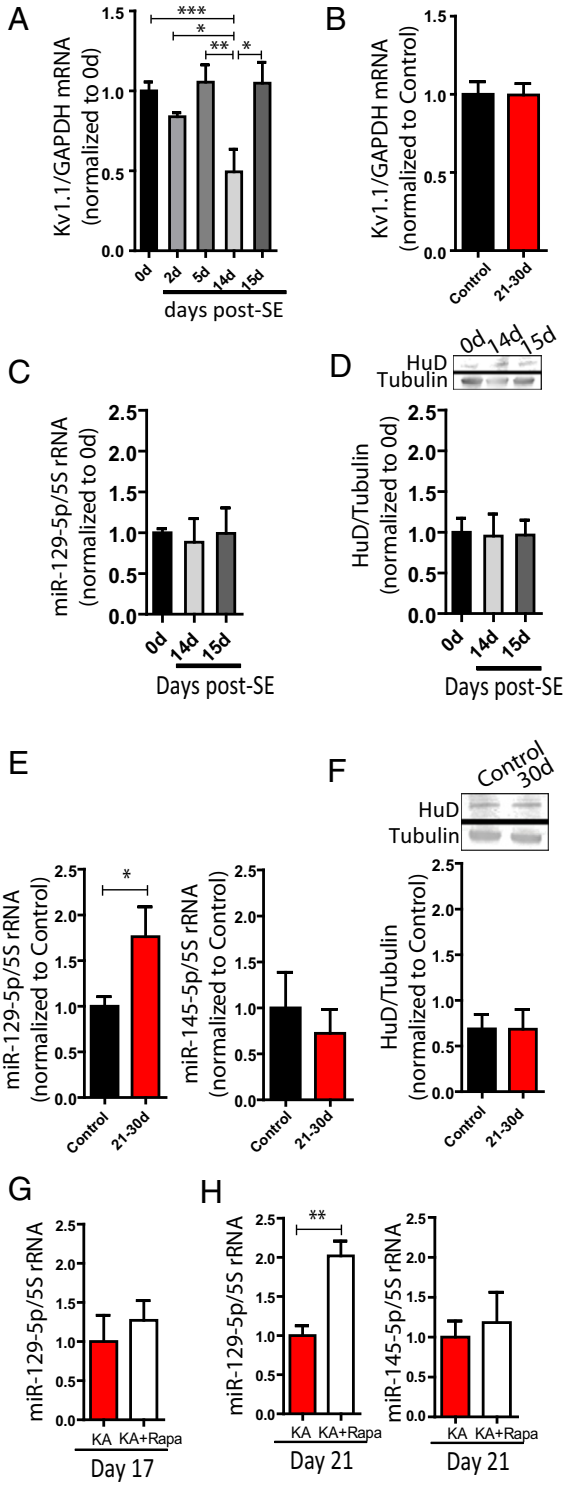

Fig. 7. miR-129-5p increases independent of mTOR activity in TLE. (A) Hippocampal SN protein was isolated from 0 day (saline + PB, euthanized 1 day post-injection) and kainic acid-(KA + PB) treated animals 2, 5, 14, and 15 days post SE. RT-qPCR was performed with specific Kv1.1 and GAPDH primers. Quantification of Kv1.1 mRNA relative to GAPDH and normalized to 0 day. 0 day: n = 14; 2 days post-SE: n = 5; 5 days post-SE: n = 5; 14 days post-SE: n = 4; 15 days post-SE: n = 3; $^{*} < 0.05$, $^{**} < 0.01$, $^{***} < 0.005$ as determined by one-way ANOVA, Newman–Keuls post hoc test. (B) Hippocampal SN protein was isolated from control (saline + PB, euthanized 21–30 days post-injection), and kainic acid-(KA + PB) treated animals 21–30 days post-SE. RT-qPCR was performed with specific Kv1.1 and GAPDH primers. Quantification of Kv1.1 mRNA relative to GAPDH and normalized to control. Control: n = 5, 21–30 days post-SE: n = 5. (C) Hippocampal SN protein was isolated from 0 day (saline + PB, euthanized 1 day post injection) and kainic acid-(KA + PB) treated animals 14 and 15 days post-SE. Quantification of miR-129-5p normalized to 5S rRNA and relative to 0 day is shown. 0 day: n = 5, 14 days post-SE: n = 4, 15 days post-SE: n = 3. Error bars represent SEM. (D) Hippocampal SN protein was isolated from 0 day (saline + PB, euthanized 1 day post-injection) and kainic acid-(KA + PB) treated animals 14 and 15 days post-SE. Top, representative Western blot of a SDS-PAGE gradient gel probed with antibodies against HuD and tubulin. Quantification of HuD signal normalized by tubulin levels and relative to 0 day. 0 day: n = 3, 14 days post-SE: n = 2, 15 days post-SE: n = 3. Error bars represent SEM. (E) Hippocampal SN protein was isolated from control (saline + PB, euthanized 21–30 days post-injection) and kainic acid-(KA + PB) treated animals 21–30 days post-SE. Quantification of miR-129-5p normalized to 5S rRNA and relative to control is shown. Right, quantification of miR-145-5p normalized to 5S rRNA is shown. Note, miR-129-5p levels are elevated 21-30 days post-SE. Control: n = 9, 21–30 days post-SE: n = 10. miR-145-5p: Control: n = 5, 21–30 day post-SE: n = 4. $^{*} < 0.05$ by Student's *t*-test. Error bars represent SEM. (F) Hippocampal SN protein was isolated from Control (saline + PB, euthanized 21–30 days post-injection) and kainic acid-(KA + PB) treated animals 21–30 days post-SE. Top, representative Western blot of a SDS-PAGE gradient gel probed with antibodies against HuD and tubulin. Quantification of HuD signal normalized by tubulin levels and relative to control. Error bars represent SEM. Control: n = 7, 21–30 days post-SE: 7. (G) Hippocampal SN protein was isolated from KA and KA + rapamycin-injected animals 17 days post-SE following timeline in Fig. 6A. Quantification of miR-129-5p normalized to 5S rRNA and relative to KA is shown. KA: n = 2, KA + Rapa: n = 2. Error bars represent SEM. (H) Hippocampal SN protein was isolated from KA and KA + rapamycin-injected animals 21 days post-SE following timeline in Fig. 6A. Quantification of miR-129-5p normalized to 5S rRNA and relative to KA is shown. KA: n = 3, KA + Rapa: n = 5. $^{**} < 0.01$ by Student's *t*-test. Error bars represent SEM.

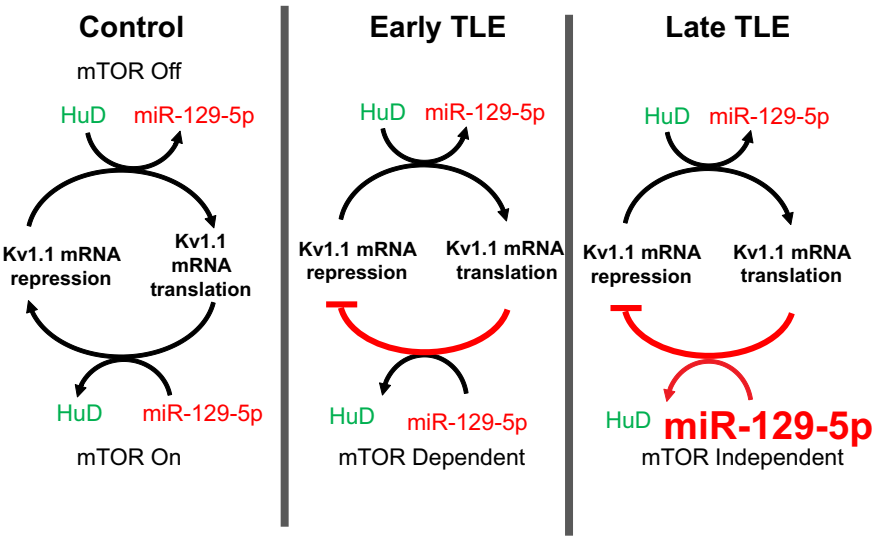

Fig. 8. Model for post-transcriptional regulation of bidirectional changes in Kv1.1 expression in TLE. At later stages of TLE (21–30 days post-SE), when mTOR activity is elevated, miR-129-5p levels increase favoring translational repression of Kv1.1 mRNA (red arrow) leading to neuronal hyperexcitability. Left panel: under conditions where mTOR activity is in equilibrium, prior to the initial status epilepticus, Kv1.1 mRNA is bound both by miR-129-5p and HuD maintaining homeostatic levels of Kv1.1. Middle panel: early in TLE, Kv1.1 expression is repressed in an mTOR-dependent manner. Right panel: late in TLE, when seizure number is significantly higher, Kv1.1 expression is repressed by an mTOR-independent mechanism and remains negatively regulated by miR-129-5p.

Alzheimer's disease (Narayanan et al., 2007; Pei and Hugon, 2008; Sharma et al., 2010; Ma et al., 2010; Zeng et al., 2011; Spilman et al., 2010).

Supplementary data to this article can be found online at http://dx.doi.org/10.1016/j.nbd.2014.09.011.

Acknowledgments

This work was supported by NSF grant #IOS 1026527 (K.R.G) and #IOS 1355158 (K.R.G.), Department of Defense USAMRMC Award W81XWH-14-1-0061 (K.R.G.) and a University of Texas Research Grant (K.R.G.). F.N. is supported by NSF PRFB 1306528. We would like to thank Dr. Daniel Johnston for his advice and critical reading of the manuscript. The authors declare no competing financial interests.

Contributions: N.S. and K.R.G designed experiments for Figs. 1–4 and 6–7. N.S. performed experiments 2–3 and 6–7. K.R.G. and D.B. designed experiment for Figs. 5 and S2. D.B. performed experiment for Figs. 5 and S2. F.N. performed experiment for Fig. 4. S.W. performed experiment for Fig. 1. K.R.G and N.S. wrote the manuscript. D.B. wrote the results section for Fig. 5. K.R.G., N.S., F. N. and D.B. edited the manuscript.

References

Aronica, E.M., Gorter, J.A., Paupard, M.C., Grooms, S.Y., Bennett, M.V., Zukin, R.S., 1997. Status epilepticus-induced alterations in metabotropic glutamate receptor expression in young and adult rats. J. Neurosci. Off. J. Soc. Neurosci. 17, 8588–8595.

Baek, J.-H., Rubinstein, M., Scheuer, T., Trimmer, J.S., 2014. Reciprocal changes in phosphorylation and methylation of mammalian brain sodium channels in response to seizures. J. Biol. Chem. 289, 15363–15373.

Baram, T.Z., 2012. The brain, seizures and epilepsy throughout life: understanding a moving target. Epilepsy Curr. Am. Epilepsy Soc. 12, 7–12.

Brewster, A.L., Lugo, J.N., Patil, V.V., Lee, W.L., Qian, Y., Vanegas, F., Anderson, A.E., 2013. Rapamycin reverses status epilepticus-induced memory deficits and dendritic damage. PLoS One 8, e57808.

Child, N.D., Benarroch, E.E., 2014. Differential distribution of voltage-gated ion channels in cortical neurons: implications for epilepsy. Neurology 82, 989–999.

Fan, Y., Fricker, D., Brager, D.H., Chen, X., Lu, H.-C., Chitwood, R.A., Johnston, D., 2005. Activity-dependent decrease of excitability in rat hippocampal neurons through increases in I(h). Nat. Neurosci. 8, 1542–1551.

Friedman, L.K., Sperber, E.F., Moshé, S.L., Bennett, M.V., Zukin, R.S., 1997. Developmental regulation of glutamate and GABA(A) receptor gene expression in rat hippocampus following kainate-induced status epilepticus. Dev. Neurosci. 19, 529–542.

Grooms, S.Y., Opitz, T., Bennett, M.V., Zukin, R.S., 2000. Status epilepticus decreases glutamate receptor 2 mRNA and protein expression in hippocampal pyramidal cells before neuronal death. Proc. Natl. Acad. Sci. U. S. A. 97, 3631–3636.

Higgs, M.H., Spain, W.J., 2011. Kv1 channels control spike threshold dynamics and spike timing in cortical pyramidal neurones. J. Physiol. 589, 5125–5142.

Hoeffer, C.A., Klann, E., 2010. mTOR signaling: at the crossroads of plasticity, memory and disease. Trends Neurosci. 33, 67–75.

Krook-Magnuson, E., Armstrong, C., Oijala, M., Soltesz, I., 2013. On-demand optogenetic control of spontaneous seizures in temporal lobe epilepsy. Nat. Commun. 4, 1376.

Lee, H.Y., Ge, W.-P., Huang, W., He, Y., Wang, G.X., Rowson-Baldwin, A., Smith, S.J., Jan, Y.N., Jan, L.Y., 2011. Bidirectional regulation of dendritic voltage-gated potassium channels by the fragile X mental retardation protein. Neuron 72, 630–642.

Lee, H., Lin, M.-C.A., Kornblum, H.I., Papazian, D.M., Nelson, S.F., 2014. Exome sequencing identifies de novo gain of function missense mutation in KCND2 in identical twins with autism and seizures that slows potassium channel inactivation. Hum. Mol. Genet. 23, 3481–3489.

Ma, T., Hoeffer, C.A., Capetillo-Zarate, E., Yu, F., Wong, H., Lin, M.T., Tampellini, D., Klann, E., Blitzer, R.D., Gouras, G.K., 2010. Dysregulation of the mTOR pathway mediates impairment of synaptic plasticity in a mouse model of Alzheimer's disease. PLoS One 5.

Matthew, E.M., Hart, L.S., Astrinidis, A., Navaraj, A., Dolloff, N.G., Dicker, D.T., Henske, E.P., El-Deiry, W.S., 2009. The p53 target Plk2 interacts with TSC proteins impacting mTOR signaling, tumor growth and chemosensitivity under hypoxic conditions. Cell Cycle (Georgetown, Tex.) 8, 4168–4175.

Meikle, L., Pollizzi, K., Egnor, A., Kramvis, I., Lane, H., Sahin, M., Kwiatkowski, D.J., 2008. Response of a neuronal model of tuberous sclerosis to mammalian target of rapamycin (mTOR) inhibitors: effects on mTORC1 and Akt signaling lead to improved survival and function. J. Neurosci. Off. J. Soc. Neurosci. 28, 5422–5432.

Meisner, N.-C., Filipowicz, W., 2011. Properties of the regulatory RNA-binding protein HuR and its role in controlling miRNA repression. Adv. Exp. Med. Biol. 700, 106–123.

Misonou, H., Menegola, M., Mohapatra, D.P., Guy, L.K., Park, K.-S., Trimmer, J.S., 2006. Bidirectional activity-dependent regulation of neuronal ion channel phosphorylation. J. Neurosci. Off. J. Soc. Neurosci. 26, 13505–13514.

Mohapatra, D.P., Misonou, H., Pan, S.-J., Held, J.E., Surmeier, D.J., Trimmer, J.S., 2009. Regulation of intrinsic excitability in hippocampal neurons by activity-dependent modulation of the KV2.1 potassium channel. Channels (Austin, Tex.) 3, 46–56.

Monaghan, M.M., Menegola, M., Vacher, H., Rhodes, K.J., Trimmer, J.S., 2008. Altered expression and localization of hippocampal A-type potassium channel subunits in the pilocarpine-induced model of temporal lobe epilepsy. Neuroscience 156, 550–562.

Narayanan, R., Johnston, D., 2010. The h current is a candidate mechanism for regulating the sliding modification threshold in a BCM-like synaptic learning rule. J. Neurophysiol. 104, 1020–1033.

Narayanan, U., Nalavadi, V., Nakamoto, M., Pallas, D.C., Ceman, S., Bassell, G.J., Warren, S.T., 2007. FMRP phosphorylation reveals an immediate-early signaling pathway triggered by group I mGluR and mediated by PP2A. J. Neurosci. Off. J. Soc. Neurosci. 27, 14349–14357.

Ozbas-Gerçeker, F., Redeker, S., Boer, K., Ozgüç, M., Saygi, S., Dalkara, T., Soylemezoglu, F., Akalan, N., Baayen, J.C., Gorter, J.A., et al., 2006. Serial analysis of gene expression in the hippocampus of patients with mesial temporal lobe epilepsy. Neuroscience 138, 457–474.

Patterson, K.P., Baram, T.Z., Shinnar, S., 2014. Origins of temporal lobe epilepsy: febrile seizures and febrile status epilepticus. Neurother. J. Am. Soc. Exp. Neurother. 11, 242–250.

Pei, J.-J., Hugon, J., 2008. mTOR-dependent signalling in Alzheimer's disease. J. Cell. Mol. Med. 12, 2525–2532.

Pfaffl, M.W., 2001. A new mathematical model for relative quantification in real-time RT-PCR. Nucleic acids research 29, e45.
Poolos, N.P., Johnston, D., 2012. Dendritic ion channelopathy in acquired epilepsy. Epilepsia 53 (Suppl. 9), 32–40.
Powell, K.L., Jones, N.C., Kennard, J.T., Ng, C., Urmaliya, V., Lau, S., Tran, A., Zheng, T., Ozturk, E., Dezsi, G., et al., 2014. HCN channelopathy and cardiac electrophysiologic dysfunction in genetic and acquired rat epilepsy models. Epilepsia 55, 609–620.
Raab-Graham, K.F., Haddick, P.C.G., Jan, Y.N., Jan, L.Y., 2006. Activity- and mTOR-dependent suppression of Kv1.1 channel mRNA translation in dendrites. Science 314, 144–148.
Racine, R.J., 1972. Modification of seizure activity by electrical stimulation. II. Motor seizure. Electroencephalogr. Clin. Neurophysiol. 32, 281–294.
Rho, J.M., Szot, P., Tempel, B.L., Schwartzkroin, P.A., 1999. Developmental seizure susceptibility of kv1.1 potassium channel knockout mice. Dev. Neurosci. 21, 320–327.
Robbins, C.A., Tempel, B.L., 2012. Kv1.1 and Kv1.2: similar channels, different seizure models. Epilepsia 53 (Suppl. 1), 134–141.
Schauwecker, P.E., Ramirez, J.J., Steward, O., 2000. Genetic dissection of the signals that induce synaptic reorganization. Exp. Neurol. 161, 139–152.
Sharma, A., Hoeffer, C.A., Takayasu, Y., Miyawaki, T., McBride, S.M., Klann, E., Zukin, R.S., 2010. Dysregulation of mTOR signaling in fragile X syndrome. J. Neurosci. Off. J. Soc. Neurosci. 30, 694–702.
Shin, M., Brager, D., Jaramillo, T.C., Johnston, D., Chetkovich, D.M., 2008. Mislocalization of h channel subunits underlies h channelopathy in temporal lobe epilepsy. Neurobiol. Dis. 32, 26–36.
Smart, S.L., Lopantsev, V., Zhang, C.L., Robbins, C.A., Wang, H., Chiu, S.Y., Schwartzkroin, P.A., Messing, A., Tempel, B.L., 1998. Deletion of the K(V)1.1 potassium channel causes epilepsy in mice. Neuron 20, 809–819.
Sosanya, N.M., Huang, P.P.C., Cacheaux, L.P., Chen, C.J., Nguyen, K., Perrone-Bizzozero, N.I., Raab-Graham, K.F., 2013. Degradation of high affinity HuD targets releases Kv1.1 mRNA from miR-129 repression by mTORC1. J. Cell Biol. 202, 53–69.
Spilman, P., Podlutskaya, N., Hart, M.J., Debnath, J., Gorostiza, O., Bredesen, D., Richardson, A., Strong, R., Galvan, V., 2010. Inhibition of mTOR by rapamycin abolishes cognitive deficits and reduces amyloid-beta levels in a mouse model of Alzheimer's disease. PLoS One 5, e9979.
Sun, H., Kosaras, B., Klein, P.M., Jensen, F.E., 2013. Mammalian target of rapamycin complex 1 activation negatively regulates Polo-like kinase 2-mediated homeostatic compensation following neonatal seizures. Proc. Natl. Acad. Sci. U. S. A. 110, 5199–5204.
Tongiorgi, E., Armellin, M., Giulianini, P.G., Bregola, G., Zucchini, S., Paradiso, B., Steward, O., Cattaneo, A., Simonato, M., 2004. Brain-derived neurotrophic factor mRNA and protein are targeted to discrete dendritic laminas by events that trigger epileptogenesis. J. Neurosci. Off. J. Soc. Neurosci. 24, 6842–6852.
Wong, M., 2012. mTOR as a potential treatment target for epilepsy. Future Neurol. 7, 537–545.
Wykes, R.C., Heeroma, J.H., Mantoan, L., Zheng, K., MacDonald, D.C., Deisseroth, K., Hashemi, K.S., Walker, M.C., Schorge, S., Kullmann, D.M., 2012. Optogenetic and potassium channel gene therapy in a rodent model of focal neocortical epilepsy. Sci. Transl. Med. 4, 161ra152.
Zeng, L.-H., Rensing, N.R., Wong, M., 2009. The mammalian target of rapamycin signaling pathway mediates epileptogenesis in a model of temporal lobe epilepsy. J. Neurosci. Off. J. Soc. Neurosci. 29, 6964–6972.
Zeng, L.-H., Rensing, N.R., Zhang, B., Gutmann, D.H., Gambello, M.J., Wong, M., 2011. Tsc2 gene inactivation causes a more severe epilepsy phenotype than Tsc1 inactivation in a mouse model of tuberous sclerosis complex. Hum. Mol. Genet. 20, 445–454 (72, 630–642).